Available online at www.sciencedirect.com
ScienceDirect
Advances in Space Research 39 (2007) 918–925
ADVANCES IN SPACE RESEARCH (a COSPAR publication)
www.elsevier.com/locate/asr

Comparison of ionospheric measurements made by digisondes with those inferred from ultraviolet airglow

R. DeMajistre [a,*], L.J. Paxton [a], D. Bilitza [b]

[a] The Johns Hopkins University, Applied Physics Laboratory, 11100 Johns Hopkins Road, Laurel, MD 20723, USA
[b] Information Technology and Scientific Services, Raytheon Technology Services Company, Lanham, MD, USA

Received 17 January 2006; received in revised form 12 June 2006; accepted 22 September 2006

Abstract

In this work we compare ionospheric measurements made at several ionosonde stations with parameters inferred from airglow measurements made by the Global Ultraviolet Imager (GUVI) instrument aboard the Thermosphere, Ionosphere, Mesosphere, Energetics, and Dynamics (TIMED) spacecraft. The purpose of this comparison is twofold. First, our study provides a validation of the technique of using TIMED/GUVI airglow measurements to infer nighttime electron densities in F region of the ionosphere. Second, we use the global characterization of the ionosphere provided by TIMED/GUVI to identify potential biases in individual ionosonde station records. We have found for peak electron densities over the range $4.0–11.0 \times 10^5$ cm^{-3} that the GUVI measurements are consistent with the ionosonde observations. We have also found some station to station and regional variations that warrant further study.

Keywords: Ionosphere; Electron density; Digisonde; Nightglow; Global observations

1. Introduction

Over the past several years, new types of measurements have become available for systematic monitoring of the ionosphere. Historically, the ionospheric characterization over much of the globe has been provided by ground based radio frequency techniques, most notably ionosondes. Capabilities are now emerging for the systematic global measurement of the ionosphere from space based platforms. The techniques include the inference of plasma densities from ultraviolet airglow measurements and Global Positioning System (GPS) occultation (see for example DeMajistre et al., 2004; Hajj and Romans, 1998). In order for these methods to be validated and established, careful comparisons with ionosonde measurements are necessary. A side benefit of these comparisons will be the ability to study the consistency of the measurements from various ionosondes from a global perspective. It should be noted that this study (and others like it) which seek to quantify the uncertainties in different types of ionospheric measurements will be important to current efforts at ionospheric data assimilation models, such as the Global Assimilation of Ionospheric Measurements (GAIM) model (Schunk et al., 2004).

In this article, we will compare night side F region plasma densities inferred from measurements made by the Global Ultraviolet Imager (GUVI) aboard the Thermosphere, Ionosphere, Mesosphere, Energetics, and Dynamics (TIMED) spacecraft with a large set of ionosonde measurements. The method of inferring F region plasma densities from the TIMED/GUVI data is given by DeMajistre et al. (2004). We will show that with a relatively small adjustment of the absolute calibration of the GUVI data that the inferred plasma densities are consistent with the aggregate set of ionosonde measurements. We will also use the GUVI data to point out some statistical anomalies in the ionosonde database.

We will first describe the ionosonde and airglow observations used to conduct this study. The results of the comparison of the data will then be presented. We will then

* Corresponding author.
E-mail addresses: robert.demajistre@jhuapl.edu, Bob.DeMajistre@jhuapl.edu (R. DeMajistre).

0273-1177/$30
doi:10.1016/j.asr.2006.09.037

draw inferences from the statistical behaviors found in the comparisons.

2. Observations

2.1. GUVI

The GUVI instrument aboard the TIMED spacecraft obtains high spatial resolution imagery in five important areas of the Far Ultraviolet (FUV) spectrum (Paxton et al., 2004). The instrument can be considered as a linear array of detectors that scan from about 500 km tangent altitude on the limb downward and then across the Earth's disk. For the analysis presented here, we use the nighttime data on the limb from the channel measuring the 135.6 nm emission from O+ recombination. DeMajistre et al. (2004) gives a full description of the inference of electron density from GUVI measurements of 135.6 nm radiance.

Fig. 1 shows the orbit ground tracks for a representative day. The limb observations yield electron density profiles roughly 17° nightward of the TIMED orbit track. The GUVI limb data are geolocated at the tangent point of the pixel with a tangent height closest to 300 km. During a single day, the observations are made at a roughly constant local time. This local time precesses with the orbit plane so that all local times are covered in a sixty-day period. Thus the GUVI night side data provide systematic global coverage of latitude once an orbit, longitude once a day, and local time every sixty days.

From Fig. 1 we see that each TIMED orbit GUVI measures a quasi-longitudinal cross section of the ionosphere. A sample ionospheric cross section is shown in Fig. 2. The figure shows the F region near equinox near local midnight during a high period of the solar cycle. The equatorial anomalies are shown seen clearly at a magnetic latitude of ±15°. These enhancements are symmetric in position but not magnitude, with a somewhat stronger southern anomaly. As illustrated by this example, the GUVI data can be a useful tool in determining the spatial structure of the ionosphere. This information is available globally and may be particularly useful in remote areas where ground based measurements are not available.

The retrieved electron densities at a given latitude can be fit to a three parameter Chapman layer function for comparison with the ionosonde measurements as illustrated in Fig. 3. In this article we will be primarily concerned with comparisons of the plasma density at the F layer maximum, the so-called NmF2, which, along with the height of the maximum and the scale height of the topside are explicit results of the Chapman layer fit. It should be noted that if the electron density profile differs significantly from the Chapman layer shape, the fit will fail, giving unreasonable values for the fitting parameters (e.g., negative heights for the layer height) or yielding unacceptably large reduced χ^2 metric (see for example Bevington and Robinson (1992)), which signals a poor fit to the data. Incidences of fitting failure are most common at higher latitudes where low plasma densities result in low signal levels and smaller signal to noise ratios. In these cases the measurement uncertainties are so large that no layer shape is apparent, and the layer height falls well below 100 km. In these cases, the reduced χ^2 is usually small because the data are not sufficient to constrain the fit. There are cases where there is sufficient signal, and the Chapman layer is not a suitable to model the data. In this case the reduced χ^2 is unacceptably large and the profile is rejected. The one sigma uncer-

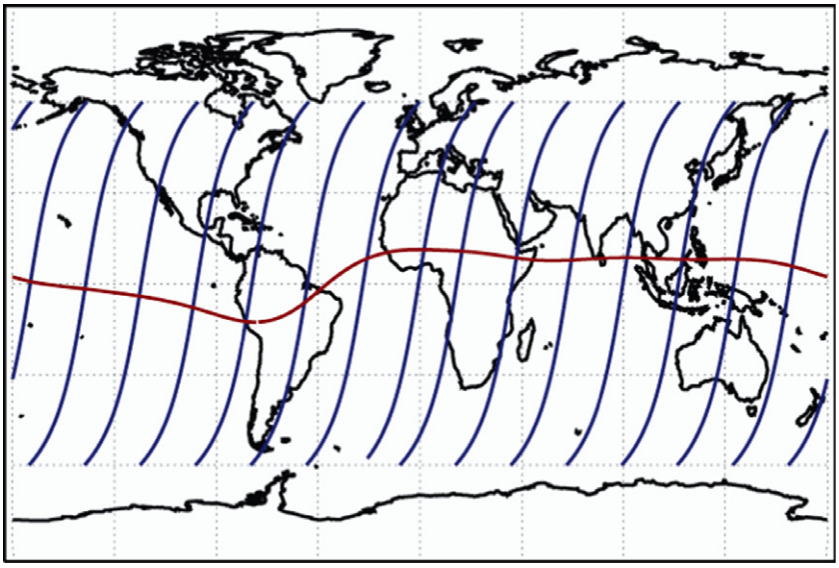

Fig. 1. TIMED spacecraft nighttime ground track for a typical day (blue traces). The magnetic equator is shown in red. The plane of the orbit moves westward and at low-mid latitudes is located within a small range of local times. (For interpretation of the references to color in this figure legend, the reader is referred to the web version of this article.)

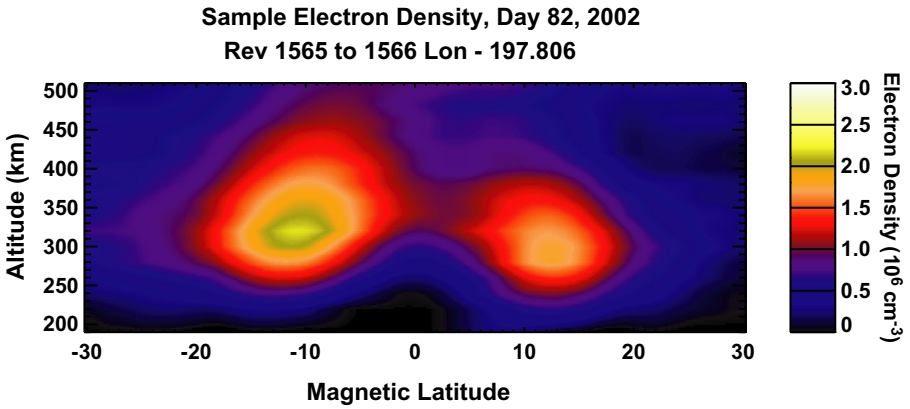

Fig. 2. Representative longitudinal cross section of the ionosphere inferred from GUVI measurement.

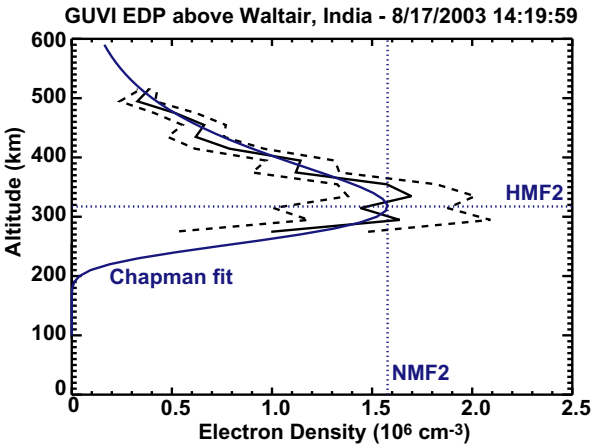

Fig. 3. Sample GUVI Electron Density Profile (EDP) with an illustration of the associated inferred ionosonde parameters. The solid black trace shows the electron density inferred from the GUVI data, while the broken black traces show the one sigma uncertainty envelope. The solid blue trace shows the best fit Chapman layer profile and the broken blue traces show the relevant Chapman layer parameters. (For interpretation of the references to color in this figure legend, the reader is referred to the web version of this article.)

tainties for NmF2 displayed below result from propagating the instrument uncertainties through the least squares fitting procedure (again see for example Bevington and Robinson (1992) for a general discussion and DeMajistre et al. (2004) for the specific procedure).

Fig. 4 shows a sample map of NmF2 for a given day derived from GUVI measurements. The figure shows the global morphology of the F region for a constant local time (near midnight) for day 89 of 2004. Such a global specification, from which can be deduced quantities such as the magnitude, separation and asymmetry of the equatorial anomalies, can be a useful tool in quantifying the factors that shape the nighttime ionosphere. However, before these data products can be used for quantitative studies, we must demonstrate that the GUVI inferences are consistent with more conventional measurements. It is our purpose here to provide such a demonstration with the ionosonde measurements.

2.2. Ionosondes and coincidence definitions

The locations of the ionosondes used in this study are plotted in Fig. 5 and a list of station names, positions, instrument types, and points of contact are given in Table 1. These measurements were acquired directly from the instrument groups themselves and in most cases have been hand scaled.

For the purpose of subsequent comparisons, we have separated the ionosonde stations into longitude sectors as shown in Fig. 5. These sectors separate the stations into longitudinally organized geographic groups. Note that although the coverage in magnetic latitude for the entire set of stations is reasonably comprehensive, the coverage in each sector is uneven. In the American sector, the southern magnetic latitudes are well covered, although there is no information from the Northern hemisphere. In the European sector, both Northern and Southern hemispheres are equally represented, but all of the data are taken at higher latitudes. The Indian and Pacific sectors have only Northern hemisphere stations, and each set of sector stations are concentrated either at lower latitudes (Indian) or higher latitudes (Pacific). For this reason it may be somewhat difficult to separate observed biases into longitudinal and latitudinal components.

Coincidences between GUVI and ionosonde stations were defined by the following conditions:

- The GUVI measurement was within 200 km and 5 min of station measurement. (The distance to the station is determined using the longitude and latitude of the GUVI tangent point near 300 km.)
- No indication of spread-F or instrument/measurement problems associated with the ionosonde measurement.
- Chapman layer fit to the GUVI data was successful.

Over the period of observation, March 2002–November of 2004, 465 coincidences were available for this study.

In order to boost the signal to noise ratio during the coincidence period, the GUVI radiance profiles were averaged within 200 km of the ionosonde station prior to deter-

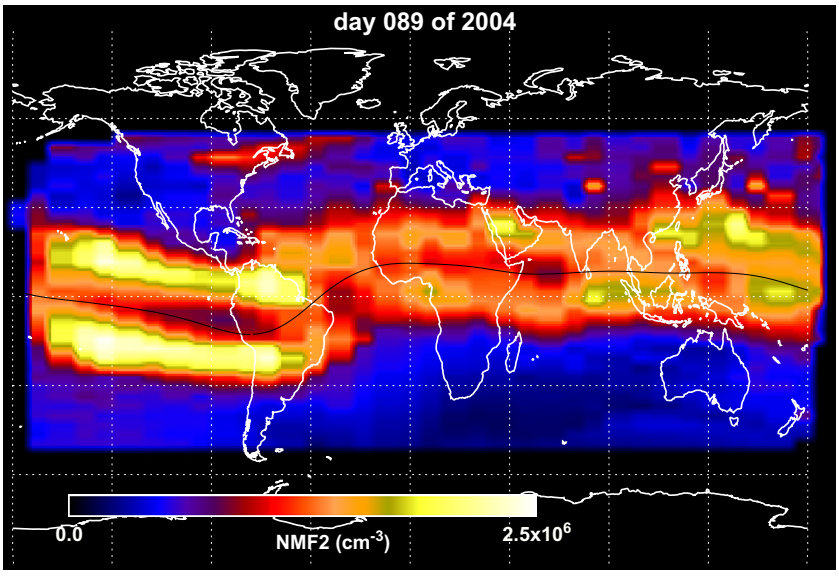

Fig. 4. Sample global map of NmF2 inferred from GUVI measurements. The GUVI observations were made at approximately midnight local time.

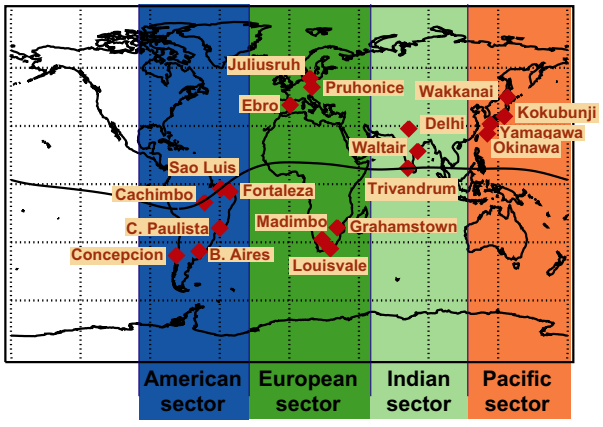

Fig. 5. Positions of ionosonde stations used in this study.

mining the electron density profiles (see Fig. 6). In practice, this usually results in the combination of two to four GUVI profiles during a single coincidence. Combining data like this significantly increased the number of successful retrievals at high latitudes where signal levels are generally low. The comparison of the data taken during these coincidences are presented next.

3. Results

The overall results of the comparisons between the GUVI inferences and the ionosonde measurements are shown in Fig. 7. In the left panel of this figure, each coincidence is marked with a small circle. The diagonal yellow line lies where the GUVI NmF2 and the ionosonde

Table 1
Ionosonde stations use in this study sorted by magnetic latitude

Station	Latitude	Longitude	Dip latitude	Instrument	Contact
Juliusruh, Germany	54.6	13.4	68.8	DPS-4	J. Mielich
Pruhonice, Czech Rep.	50	14.6	66.5	DPS-4	D. Buresova
Wakkanai, Japan	45.0	141.0	59.6	Own design	T. Maruyama
Ebro, Spain	40.8	0.5	55.7	DGS256	D. Altadill
Kokubunji, Japan	35.0	139.0	48.4	Own design	T. Maruyama
Yamagawa, Japan	31.0	130.0	44.2	Own design	T. Maruyama
Delhi, India	28.6	77.2	42.6	KEL IPS71	R. S. Dabas
Okinawa, Japan	26.0	128.0	36.5	Own design	T. Maruyama
Waltair, India	17.0	83.0	20.2	–	K. Niranjan
Trivandrum, India	8.3	76.6	0.3	KEL, Man. S.	C. Devasia
Sao Luis, Brazil	−2.3	315.8	−0.5	DGS256	I. Badista
Cachimbo, Brazil	−9.5	305.2	−3.2	DPS	I. Badista
Fortaleza, Brazil	−3.9	321.5	−9.0	DPS-4	I. Badista
C. Paulista, Brazil	−22.7	315.0	−28.0	DGS256	I. Badista
B. Aires, Argentina	−34.6	301.7	−37.2	–	M. Mosert
Concepcion, Chile	−36.8	287.0	−37.5	IPS42	A. Foppiano
Madimbo, SA	−22.4	30.9	−58.1	DPS	L. McKinnell
Grahamstown, SA	−33.3	26.5	−63.1	DPS	L. McKinnell
Louisvale, SA	−28.5	21.2	−63.1	DPS	L. McKinnell

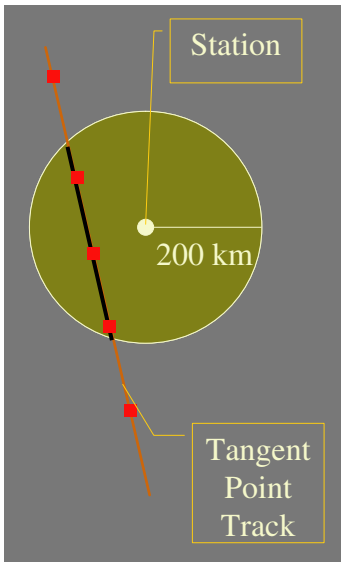

Fig. 6. Coincidence definition. Note that the tangent point is the position where the GUVI line of sight is closest to the Earth. The tangent point track is the ground track of the tangent point of the GUVI pixel that is closest to 300 km.

NmF2 are in perfect agreement. From the figure we see that the measurements are clearly correlated, particularly in the region below 1×10^6 cm^{-3}. In order to quantify the agreement between the data sets, we binned the coincidences according to the ionosonde NmF2 value. For ionosonde NmF2 values less than 1.2×10^6 cm^{-3} we chose bin widths of 1.0×10^5 cm^{-3}. For larger values of NmF2, where fewer coincidences were available, the bin size was increased to 2.0×10^5 cm^{-3}. A mean and standard deviation was computed for all of the coincident GUVI inferences within each bin. The mean values and the standard deviation envelope are shown with the red traces.

The right panel of Fig. 7 shows the fractional error and standard deviation of the GUVI NmF2 with respect to the ionosonde measurements. The solid black trace on the right is essentially the red trace on the left expressed as a fraction of ionosonde NmF2. The broken black lines show the standard deviation envelope in a similar representation. This panel directly expresses the systematic and statistical differences between the GUVI and ionosonde NmF2 values. For example, were an ionosonde to measure an NmF2 value of (0.8×10^6 cm^{-3}), we should expect GUVI, on average and within about 30% to be very similar to the ionosonde. If instead, the ionosonde measures 0.4×10^6 or 1.2×10^6 we should expect the GUVI NmF2 to be 30% high or 20% low, respectively, (again within about 30% of statistical variation). In short, the solid black line shows the amount that the GUVI should be adjusted to be statistically consistent with the ionosonde measurements.

The cause of the bias at low values of NmF2 is well understood and arises from the lack of signal from the 135.6 nm emission in the GUVI instrument (DeMajistre et al., 2004). The bias arises from the requirement that the volume emission rates (which is approximately the square of the electron density) be everywhere positive. Under such conditions an average volume emission rate of zero is not possible, and a positive bias is introduced. At values of NmF2 larger than about 1.1×10^6 the agreement between the ionosonde data and the GUVI inferences is much less compelling. The reason(s) for this disagreement are unclear and are discussed below.

Fig. 8 shows the coincidence data from each station along with the global statistics for comparison. In this figure, the station data are shown with the green diamonds. The stations in the figure follow the order given in Table 1, that is, in order of decreasing magnetic latitude. From the figure we see a noticeable variation of the coincidence statistics from station to station. For example, the ionosonde NmF2 observations at Delhi are systematically much higher than the GUVI inferences. This is to be compared with the measurements at Yamagawa and Okinawa, both at magnetic latitudes similar to Delhi, which show

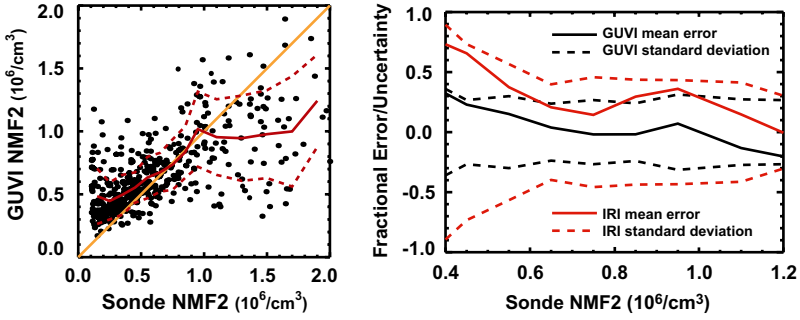

Fig. 7. Global comparison between GUVI inferred NmF2 and ionosonde measurements. The left panel shows a scatter plot of the GUVI NmF2 vs. the ionosonde NmF2 (small circles). Also shown on the left side are the binned average NmF2 (solid red trace) along with its associated standard deviation (broken red trace). See the text for a more detailed description of the red traces on the left panel of the figure. The right panel shows the average fractional error of the GUVI NmF2 with respect to the ionosonde NmF2 (solid black) along with the standard deviation (broken black) corresponding to the statistical uncertainty. Also shown in red are the same quantities using the International Reference Ionosphere (IRI) (Bilitza, 2001) in place of the GUVI data. Note that the scale for the right panel is restricted to the range 0.4–1.2 $\times 10^6$ where the global data shows good agreement. (For interpretation of the references to color in this figure legend, the reader is referred to the web version of this article.)

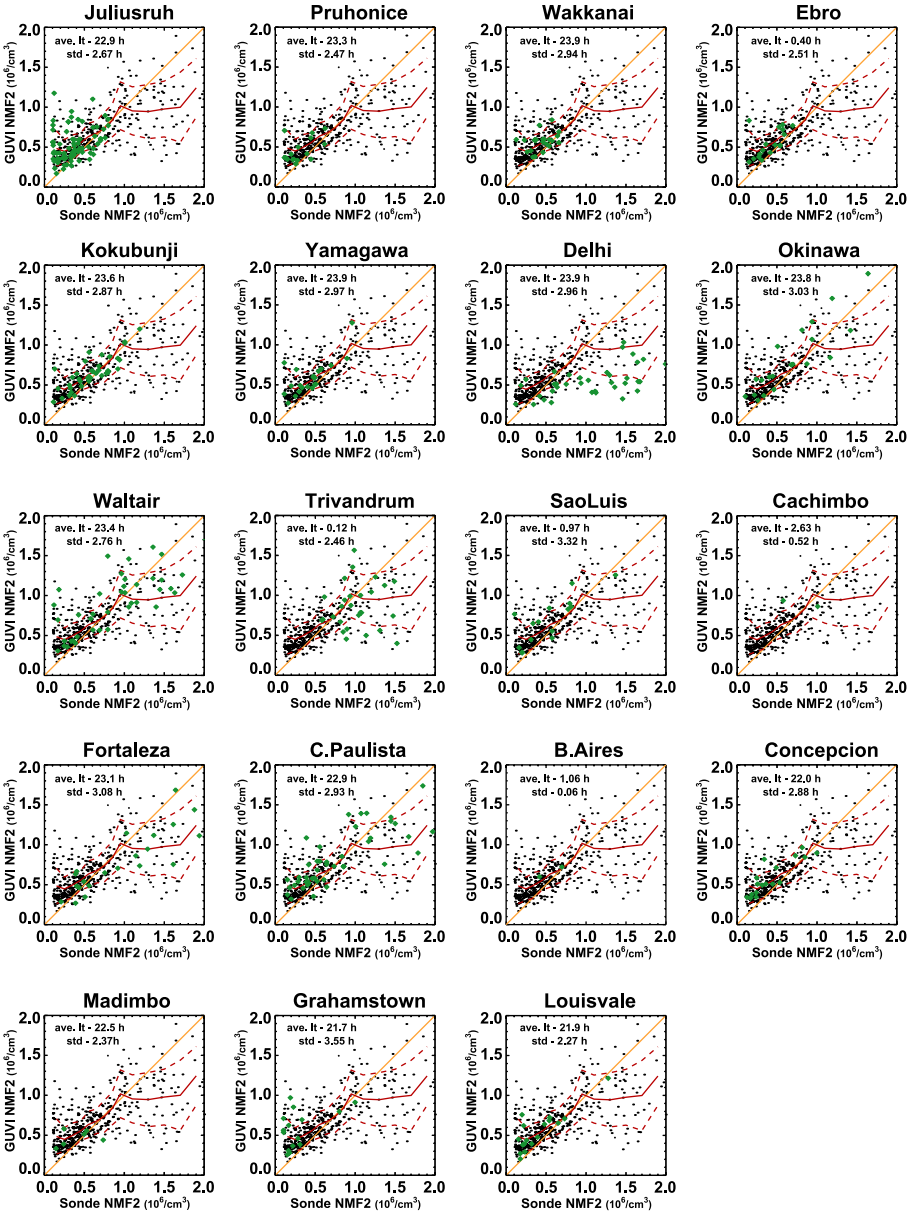

Fig. 8. Station by station statistics for the NmF2 comparison. Each one of the panels shows the data from an individual station, shown with green diamonds over the left panel of Fig. 7. Also shown in each panel is the average and standard deviation of the local times for the coincidences at each station. (For interpretation of the references to color in this figure legend, the reader is referred to the web version of this article.)

rather good agreement with the GUVI inferences. Even without the Delhi data, however, the GUVI inferences at NmF2 levels ($>1.1\times10^6$ cm^{-3}) remain systematically low. There are also large variations in the spread of the measurements from station to station. For example, the ionosonde measurements at Trivandrum show very little correlation with the GUVI inferences. The inferences from above Sao Luis, which is also very near the magnetic equator, however, shows a rather tight correlation with the measurements.

Note that we have included the average and standard deviation of the local time of observation for each of the stations. For the stations with a significant number of measurements, the average observation time is within and hour or so of local midnight. The notable exception is the South African stations for which the average time is closer to 22H. In view of these statistics, we may safely conclude that any local time biases in the station data may be safely neglected.

Fig. 9 shows the behavior of the coincidence correlation according to geographic region. The data are separated into magnetic latitude regions and color coded by longitude sector. Also shown on the figure are the means and standard deviation envelopes calculated for each latitude region. Overall, there is little evidence for changes in the statistics based on geomagnetic latitude. The means and standard deviations for each latitude region are quite similar to the global statistics.

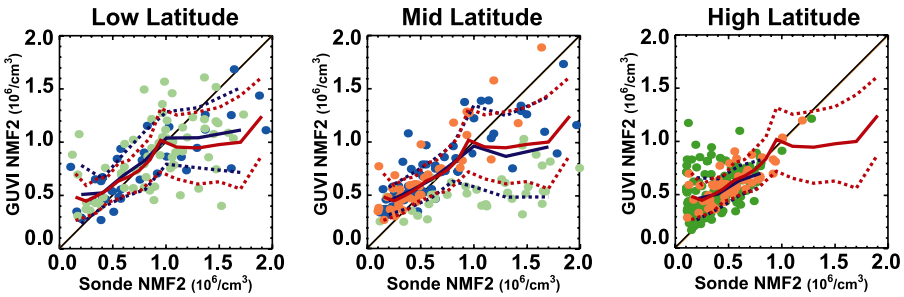

Fig. 9. GUVI/ionosonde comparison grouped by latitude and region. Each panel shows the data from a given range of magnetic latitude, low ($< |20°|$), mid ($\geqslant |20°|$ and $< |45°|$) and high ($\geqslant |45°|$). Each point is color coded with its longitude sector using the colors in Figure 5. Again, the red traces show the global means and standard deviations. The blue traces show the averaged statistics for the corresponding latitude regions. (For interpretation of the references to color in this figure legend, the reader is referred to the web version of this article.)

There are, however, clear longitudinal differences. The high latitude data are drawn exclusively from the European and Pacific sectors. Although the mean values look quite similar for each set of color coded points, the European sector data exhibit much more spread about the diagonal. In the mid-latitudes, we see that although the statistics for the American and Pacific sectors look consistent with one another. The Indian data are systematically higher than the GUVI inferences. This is due to the previously noted anomaly in the statistics from the Delhi station since the mid-latitude data from the Indian sector is provided by the station at Delhi exclusively. At low latitudes, only data from the American and Indian sectors are available. The statistics in this region look reasonably consistent with one another. The slightly larger spread in the Indian data are due to the previously noted anomalous standard deviation in the data from Trivandrum.

4. Discussion and conclusion

All in all, we find good systematic agreement of the GUVI inferences with the ionosonde data with a standard deviation of about 30% for NmF2 values in the range $4.0–11.0 \times 10^5\ \mathrm{cm}^{-3}$. There are, however, some regional differences in the statistics of the comparisons.

The source of the regional differences is not immediately evident. The variation in the comparison statistics may originate from problems with the GUVI inferences of NmF2 or inconsistency in the measurement or interpretation of the ionograms at the various ground stations. These possible sources of the regional differences will be discussed in turn.

Since all of the GUVI measurements are made with the same instrument and the calibration of the instrument has been shown to be stable over the period of the observations, it is unlikely that the regional differences are caused by the radiance measurements underlying the GUVI NmF2 inferences. If the GUVI inferences are subject to regional variations then the source of these variations must be the assumptions made during the process of inferring NmF2. The three most critical assumptions made during the inference process are (1) Chapman-like shape of the electron density profile, (2) horizontal homogeneity over the line of sight, and (3) electron temperature in the F region. One would think that if the quality of these assumptions was regionally variable, that such variability would exhibit itself as a function of geomagnetic latitude, since the structure of the ionosphere is primarily latitudinal in nature. According to Fig. 9, however, there is very little evidence of variability in the statistics as a function of latitude. We note that the average magnitude of the NmF2 does, of course, vary with latitude, but the quality of the comparison between the GUVI inferences and the ionosonde measurements does not. Thus, if the GUVI inferences are inconsistent, there must be some longitudinal variation in the structure of the ionosphere that modifies the inferences.

Kil et al. (2004) present some of the characteristic variations of the ionosphere as a function of longitude and season. Sagawa et al. (2005) also present evidence of longitudinal variations in the nighttime ionosphere that may be related to tidal structures in the thermosphere. Kil et al. (2004) note that some of these changes, particularly in the equatorial ionization anomalies, can be related to the occurrence of plasma irregularities associated with so-called spread-F. These irregularities could certainly present problems to the extraction of GUVI profiles. However, all coincidence events that were annotated by the ionosonde operator as having spread-F present were excluded by the retrieval. It is also unusual that the effects of these irregularities on the GUVI inferences would not exhibit more evident latitudinal dependence. Clearly a more careful study of the performance of the GUVI algorithms in the presence of plasma irregularities needs to be undertaken.

As an alternative to the as yet unspecified longitudinal bias in the GUVI inferences, there may be station to station or regional differences in the data from the ionosondes. These are different instruments operated by different institutions hand scaled by different individuals. They are generally not inter-calibrated with one another. Although the frequency calibration and determination of NmF2 from an ionogram is a straightforward process, there may, nonetheless arise statistical inconsistencies. Another possible source of problems may lie in the management of the data

at individual stations. Processes such as time tagging and archive management may introduce errors in NmF2 assignment. In the absence of independent validation, these problems can go undetected.

Inferences of NmF2 from orbit can help to identify problems at individual stations or regions. Plots like those in Fig. 8 show obvious statistical discrepancies between the comparisons at various stations. Plots of this type can be made for one station at different times as well (in order to study the stability of a data set when changes are made to a station's instrumentation or data processing). Since direct inter-calibration of the facilities is not an option, comparison with a single orbiting instrument offers a convenient alternative. It may not be possible to identify the source of discrepancies with this type of comparison, but anomalies can certainly be identified.

At this point, it is unclear whether the discrepancies shown in Fig. 8 result from station to station variation in the ionosonde data or some sort of longitudinal variation in the structure of the ionosphere that modifies the inferences NmF2 by GUVI. In either case, this comparison points towards useful information. If the GUVI data are variable, it is due to a non-obvious characteristic the ionosphere, the determination of which would advance our understanding of the region. If the cause is truly station to station variability in the ionosonde record, then the statistical information in Fig. 8 can be used to correct the problems at the individual facilities.

In conclusion, we have found that the GUVI inferences of NmF2 are globally consistent with ionosonde measurements within the range $4.0–11.0 \times 10^5\ \mathrm{cm}^{-3}$. There are, however, some statistical discrepancies of uncertain origin that warrant further study, particularly at larger values of NmF2.

Acknowledgements

The authors thank the providers of the ionosonde data, D. Altadill, I. Badista, D. Buresova, R.S. Dabas, C. Devasia, A. Foppiano, T. Maruyama, L. McKinnell, J. Mielich, M. Mosert, and K. Niranjan for their contribution to this work.

References

Bevington, P., Robinson, D. Data Reduction and Error Analysis for the Physical Sciences, second ed McGraw-Hill, New York, 1992.

Bilitza, D. International reference ionosphere 2000. Radio Sci. 36, 261–275, 2001.

DeMajistre, R., Paxton, L., Morrison, D., Yee, J.-H., Goncharenko, L., Christensen, A., 2004. Retrievals of nighttime electron density from TIMED Global Ultraviolet Imager (GUVI) measurements. J. Geophys. Res. 109, Article A05305.

Hajj, G.A., Romans, L.J. Ionospheric electron density profiles obtained with the global positioning system: results from the GPS/MET experiment. Radio Sci. 33, 175–190, 1998.

Kil, H., DeMajistre, R., Paxton, L., 2004. F-region plasma distribution seen from TIMED/GUVI and its relation to the equatorial spread F activity. Geophys. Res. Lett. 31, Article L05810.

Paxton, L.J., Christensen, A., Morrison, D., Wolven, B., Kil, H., Zhang, Y., Ogorzalek, B., Humm, D., Goldsten, J., DeMajistre, R., Meng, C.-I. GUVI: a hyperspectral imager for geospace, in: Nardell, C., Lucey, P., Yee, J.-H., Garvin, J. (Eds.), Instruments, Science and Methods for Geospace and Planetary Remote Sensing. SPIE–the International Society for Optical Engineering. Bellingham, WA, pp. 228–240, 2004.

Sagawa, E., Immel, T., Frey, H., Mende, S., 2005. Longitudinal structure of the equatorial anomaly in the nighttime ionosphere observed by IMAGE/FUV. J. Geophys. Res. 110, Article A11302.

Schunk, R., Scherliess, L., Sojka, J.J., Thompson, D.C., Anderson, D.N., Codrescu, M., Minter, C., Fuller-Rowell, T.J., Heelis, R.A., Hairston, M., Howe, B., 2004. Global assimilation of ionospheric measurements (GAIM). Radio Sci. 39, Article RS1S02.